J|A|C|S
ARTICLES
Published on Web 07/28/2004

Xe Chemical Shift Tensor in Silicalite and SSZ-24

Cynthia J. Jameson

Contribution from the Department of Chemistry, M/C-111, University of Illinois at Chicago, 845 West Taylor, Chicago, Illinois 60607-7061

Received January 9, 2004; Revised Manuscript Received March 8, 2004; E-mail: cjjames@uic.edu

Abstract: We report, for the first time, a theoretical prediction of the ^{129}Xe nuclear magnetic resonance chemical shift tensor of xenon atom in a single crystal of silicalite at near-zero occupancy and the temperature dependence of the Xe NMR chemical shift tensor for the polycrystalline silicalite at maximum occupancy. The former is a measure of the sensitivity of the Xe tensor components to the local structure of the channels without Xe−Xe contributions. The latter is a measure of the sensitivity of the Xe−Xe tensor components to the Xe−Xe distributions, as determined by the Xe−Xe potential function in competition with the Xe−silicalite potential function. Both theoretical predictions can be compared against Xe NMR experiments: the first against the Xe spectra collected as a function of rotation of the single crystal about the three crystalline axes in a magnetic field, and the second against variable temperature Xe NMR studies (below room temperature) of polycrystalline silicalite at maximum Xe occupancy. With the same parameter set (Xe−O potential and shielding functions), we predict the line shapes of Xe in SSZ-24 zeolite under various conditions of occupancy and temperature.

1. Introduction

Xe NMR spectroscopy has proven to be a very useful tool for studying catalytic materials, polymers, molecular crystals, biological systems, and even tissues of live animals.[1,2] The exquisite sensitivity of the Xe chemical shift to the immediate environment of the Xe atom is the basis for these applications which have become even more significant with the enhanced sensitivity provided by hyperpolarized Xe.[3] In addition to the isotropic chemical shift, which is the usual observed quantity, especially in solution and in biological materials, the Xe chemical shift tensor for Xe trapped in cages and diffusing through channels can be observed, under the proper conditions.[4−14] The more complete information provided by the chemical shift tensor poses a challenge to our understanding of the nature of the dynamic averaging that is going on and the nature of the environments that encapsulate the Xe atoms.

The first Xe NMR spectra in a single-crystal experiment have been reported by Terskikh et al. using hyperpolarized ^{129}Xe in a single crystal of silicalite.[14] These definitive experiments provide, for the first time, a complete set of dynamically averaged tensor components for a single Xe atom in the adsorbed state. Our earlier NMR studies of Xe in silicalite provided anisotropic line shapes at 300, 270, and 240 K in the larger crystals at maximum occupancy.[11] The recent studies reported anisotropic line shapes at full occupancy as a function of temperature at 160, 150, and 140 K. In the recent work, the progression of line shape changes, from low occupancy at room temperature to higher occupancy at lower temperatures, exhibits one apparently unchanging tensor component,[14] which also had been a point of curiosity noted in the earlier studies below room temperature.[11]

In this paper we report grand canonical Monte Carlo (GCMC) simulations of the Xe chemical shift in a silicalite crystal as a function of orientation with respect to the magnetic field, which effectively mimic all the experimental findings. The calculations make use of the dimer tensor model and the same Xe−O shielding function and Xe−O potential parameters throughout, to provide not only the rotation patterns of the single-crystal experiment at 295 K[14] but also the line shapes in the Xe spectra as a function of temperature for the polycrystalline silicalite at maximum occupancy.[11,14] The agreement with experiments is semiquantitative, and all the qualitative trends observed experimentally are reproduced by the calculations in the present work.

2. Methods

The methods used in the GCMC simulations of the line shapes have been described earlier.[15,16] The same calculations had produced as standard output the rotation patterns for Xe in ALPO-11, SSZ-24, and

(1) Ratcliffe, C. I. *Annu. Rep. NMR Spectrosc.* **1998**, *36*, 123−221.
(2) Bonardet, J. L.; Fraissard, J.; Gedeon, A.; Springuel-Huet, M. A. *Catal. Rev.—Sci. Eng.* **1999**, *41*, 115−225.
(3) Goodson, B. M. *J. Magn. Reson.* **2002**, *155*, 157−216.
(4) Davidson, D. W.; Handa, Y. P.; Ripmeester, J. A. *J. Phys. Chem.* **1986**, *90*, 6549−6552.
(5) Ripmeester, J. A.; Ratcliffe, C. I.; Tse, J. S. *Trans. Faraday Soc. 1* **1988**, *84*, 3731−3745.
(6) Lee, F.; Gabe, E.; Tse, J. S.; Ripmeester, J. A. *J. Am. Chem. Soc.* **1988**, *110*, 6014−6019.
(7) Springuel-Huet, M. A.; Fraissard, J. *Chem. Phys. Lett.* **1989**, 299−302.
(8) Ripmeester, J. A.; Ratcliffe, C. I. *J. Phys. Chem.* **1990**, *94*, 8773−8776.
(9) Collins, M. J.; Ratcliffe, C. I.; Ripmeester, J. A. *J. Phys. Chem.* **1990**, *94*, 157−162.
(10) Ripmeester, J. A.; Ratcliffe, C. I. *J. Phys. Chem.* **1995**, *99*, 619−622.
(11) Jameson, C. J.; Jameson, A. K.; Gerald, R. E., II; Lim, H. M. *J. Phys. Chem. B* **1997**, *101*, 8418−8437.
(12) Sozzani, P.; Comotti, A.; Simonutti, R.; Meersman, T.; Logan, J. W.; Pines, A. *Angew. Chem., Int. Ed.* **2000**, *39*, 2695−2698.
(13) Meersmann, T.; Logan, J. W.; Simonutti, R.; Caldarelli, S.; Comotti, A.; Sozzani, P.; Kaiser, L. G.; Pines, A. *J. Phys. Chem. A* **2000**, *104*, 11665−11670.
(14) Terskikh, V. V.; Moudrakovski, I. L.; Du, H.; Ratcliffe, C. I. Ripmeester, J. A. *J. Am. Chem. Soc.* **2001**, *123*, 10399−10400.
(15) Jameson, C. J. *J. Chem. Phys.* **2002**, *116*, 8912−8929.

10.1021/ja040012a CCC: $27.50

Xe in the clathrate hydrates (structures I, II, H, and bromine hydrate), but this is the first time that experiments have been available for comparison. Briefly, the method relies on the dimer tensor model[15] which considers the contributions to intermolecular Xe shielding as additive and derived from the Xe−O dimer parallel and perpendicular tensor components, which are assumed to be known. Typically we obtain the dimer tensor components via quantum mechanical calculations on Xe in model systems having the same electronic structure as the atoms constituting the channels (in these particular examples the channel atoms are bridging O atoms) and then fitting to an interpolating functional form in inverse powers of the distance (−6 to −12, usually) that reproduces the quantum mechanically calculated values of Xe tensor components and permits the calculation of the Xe tensor components at arbitrary locations between these. For example, in zeolite NaA, the ab initio calculations used several fragments of the alpha cage (including the Na^+ ions) in the NaA zeolite.[17] In the case of the clathrate hydrates,[16] the ab initio and density functional calculations used model systems consisting of cage water molecules plus the entire set of hydrogen bonding partners of the cage waters fully treated in all-electron calculations, in the presence of the remaining oxygen and hydrogen atoms of the infinite crystal represented by a self-consistent set of point charges. The array of point charges is determined by reproducing the Madelung potential at the location of the Xe atom. For Xe in the cryptophane cages, we find the five Xe-site dimer functions by doing quantum mechanical Xe shielding calculations for Xe in various positions in the half-cage.[18] For ALPO-11 we investigated several Xe−O dimer functions,[15] one of which we use in the present work.

Given the Xe−O dimer shielding parallel and perpendicular functions, the *xx*, *xy*, *yy*, etc. components of the Xe shielding tensor for a given Xe atom within the channel can be calculated for any arbitrary positions of any number of Xe atoms, since the Xe−Xe dimer tensor functions are also known from ab initio or density functional calculations. The equations that relate the dimer parallel and perpendicular components to their contributions to *xx*, *xy*, etc. components have been derived previously.[15,16] The binning of the Xe resonance frequencies (or their equivalent shielding values) for various directions of magnetic field relative to the crystal frame, under fast or slow diffusion, has been described.[15] The grand canonical Monte Carlo scheme itself, as it is implemented in our work, has been described earlier.[19] In our GCMC scheme, the Mezei cavity-biased method[20] has been used in addition to the standard Norman−Filinov scheme,[21] in order to have more efficient sampling of configurations when the channels are crowded with Xe atoms, which is especially important in this work at half- to full-occupancy conditions. Our simulation box for silicalite consisted of 2 × 2 × 2 unit cells under periodic boundary conditions.

Pairwise additive potential functions were used for both Xe−Xe and Xe−O. The Xe−Xe potential is the same one as we have always used for simulations,[19] a Maitland−Smith[22] form fitted to the Aziz−Slaman empirical potential that reproduces available data for Xe−Xe including vibrational spectra.[23] The Maitland−Smith function is of the form

$$V = \epsilon\left\{\frac{6}{n-6}\bar{r}^{-n} - \frac{n}{n-6}\bar{r}^{-6}\right\}$$

where n is allowed to vary with $\bar{r} = r/r_{min}$ according to $n = m + \gamma(\bar{r} - 1)$. For Xe−Xe, $m = 13$, $\gamma = 11$, $r_{min} = 4.3627$ Å, and $\epsilon/k_B = 282.29$ K. The same Xe−O potential is used throughout, as was used in our earlier simulations in silicalite,[11] which reproduces the adsorption isotherms of silicalite,[24,25] a Lennard-Jones function with $r_0 = 3.7$ Å, and $\epsilon/k_B = 130$ K. A better Xe−O potential could be obtained by optimizing the parameters starting from the Maitland−Smith form of the Xe−Ar potential function. However, the goal of the present work is not to fit the experiment, but rather to use the same shielding and potential functions we have used previously for simulations in silicalite[11] to see whether we can understand the Xe tensor information yielded up by the new experiments.

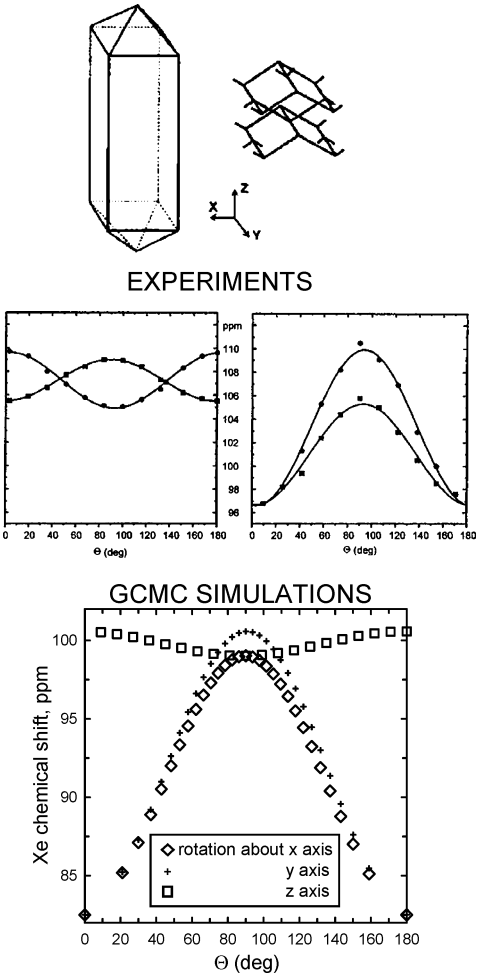

Figure 1. Rotation NMR spectra of ^{129}Xe calculated in a simulation box of 2 × 2 × 2 unit cells under periodic boundary conditions at 300 K (this work), compared with the observed results in a single crystal of silicalite at 295 K from ref 14 (reproduced with permission from the American Chemical Society). The *x*, *y*, *z* coordinate system, used in the indices of the tensor components and the axes about which the mounted crystal is rotated in the GCMC simulations, is according to the definition in ref 14, shown relative to the crystal faces, with the *y* axis along the direction of the straight channels. The calculated average values for the three components are $\delta_{xx} = 100.6$, $\delta_{yy} = 99.0$, and $\delta_{zz} = 82.5$ ppm.

3. Results

a. Silicalite. The results at very low occupancy of Xe in silicalite (0.285 Xe/unit cell) at 300 K are shown in Figure 1, where they are compared with the experimental rotation patterns. We show our patterns for rotation of the single crystal around the same axes as experiment. In our simulations, the *y* axis is the direction along the straight channels of the silicalite, the same *y* axis as drawn for the crystal in Figure 1. In single-

(16) Jameson, C. J.; Stueber, D. *J. Chem. Phys.* **2004**, *120*, 10200−10214.
(17) Jameson, C. J.; Lim, H. M. *J. Chem. Phys.* **1995**, *103*, 3885−3894.
(18) Sears, D. N.; Jameson, C. J. *J. Chem. Phys.* **2003**, *119*, 12231−12244.
(19) Jameson, C. J.; Jameson, A. K.; Baello, B. I.; Lim, H. M. *J. Chem. Phys.* **1994**, *100*, 5965−5976.
(20) Mezei, M. *Mol. Phys.* **1980**, *40*, 901−906.
(21) Norman, G. E.; Filinov, V. S. *High Temp. USSR* **1969**, *7*, 216.
(22) Maitland, G. C.; Rigby, M.; Smith, E. B.; Wakeham, W. A. *Intermolecular Forces, Their Origin and Determination*; Clarendon Press: Oxford, 1981.
(23) Aziz, R. A.; Slaman, M. *J. Mol. Phys.* **1986**, *57*, 825−841.
(24) Tsiao, C.; Corbin, D. R.; Durante, V.; Walker, D.; Dybowski, C. *J. Phys. Chem.* **1990**, *94*, 4195−4198.
(25) Bülow, M.; Hartel, U.; Müller, U.; Unger, K. K. *Ber. Bunsen-Ges. Phys. Chem.* **1990**, *94*, 74−76.

crystal experiments the *xx*, *yy*, and *zz* components from the spectra are identified with respect to the crystal frame, of course. In this particular experiment, the twinned crystal provides the signals from both elements of the twin, while we see only one set when we use the coordinates of the perfect crystal, based on the diffraction data. As discussed in the experimental paper, the relative orientation of the twins is 90° around the *z* axis, with *x* and *y* axes swapped. For the purpose of the comparison in Figure 1, we just need to note that the two patterns published for rotation about the *x* axis are also the identical patterns observed for rotation about the *y* axis. Thus, to select one of the twin elements, we pick out one of the sets of peaks from each of three figures, the latter two of which are identical, so only one is shown.

We see in Figure 1 that we have essential agreement with the experiment in terms of the number of unique principal components and their relative magnitudes, and the absolute Xe chemical shifts with respect to a free Xe atom are reasonably close to experiment. The smallest chemical shift component is along the *z* axis, which is uniquely identified in the experiment, and the middle sized tensor component is now identified as along the direction of the straight channels, the *y* axis. The prediction of the order of the components in the nearly empty silicalite, $\delta_{xx} > \delta_{yy} > \delta_{zz}$, where *x*, *y*, and *z* correspond to the crystal frame axes shown in Figure 1, is robust and remains unchanged when using a different potential function for Xe−O. It has been found in our previous work that the relative order of the Xe tensor components in the nearly empty crystal is a property of the channel architecture.[15] In this particular case, where the tensor is a general tensor with six components, the simulations also provide the off-diagonal tensor components, $(1/2)(\delta_{xy} + \delta_{yx})$, etc., although these are small in this case (as also found experimentally in ref 14) and within the statistical errors of the simulation. Both experiments and theoretical calculations agree that the anisotropy of a single Xe atom in silicalite is not very large. Experiment gives the span = 13.15 ± 0.35 ppm; the simulations result in span = 18.1 ppm.

We also calculated line shapes for the silicalite at maximum occupancy (16 Xe atoms per unit cell) at two temperatures in the polycrystalline material. We show the ^{129}Xe NMR line shapes for 300 and 150 K in Figure 2. Each of the three singularities (smoothed over by line broadening) in the spectrum corresponds to a tensor component. We see that we have essential agreement with experiments reported from two laboratories.[11,14] With decreasing temperature, at full occupancy, experiments show the two larger components (now assigned as δ_{xx} and δ_{zz}) are greatly increasing in magnitude and the smallest component (now assigned as δ_{yy}) is changing the least. Both sets of experiments[11,14] reported the smallest component remaining approximately unchanged with decreasing temperature, but the tensor components were unassigned in these experiments. The present simulations permit the assignment of the three components of the Xe shielding tensor in the fully occupied silicalite. In terms of the chemical shifts, the order at 300 K and at 150 K is $\delta_{zz} > \delta_{xx} > \delta_{yy}$. The relative order of the tensor components arising from the Xe−Xe contributions is also a property of the channel architecture.[15] Thus, so long as the magnitudes of the Xe−Xe and Xe−O contributions relative to each other are reasonably well represented by calculations, the predicted relative order of the overall Xe tensor components in the fully occupied silicalite should be correct. In the particular case of silicalite, if a somewhat different Xe−O potential is used, the relative order of the tensor components remains unchanged. At 150 K the experimental span is about 40 ppm;[14] the simulations give a span of $\delta_{zz} - \delta_{yy} = 41.2$ ppm. At 300 K the experimental span is 24.4 ppm,[11] while the simulations yield $\delta_{zz} - \delta_{yy} = 26.8$ ppm. In going from 300 to 150 K the calculated δ_{yy} component changed the least for the fully occupied silicalite. Thus, with increasing occupancy at 300 K, the relative order of the calculated chemical shift tensor components go from $\delta_{xx} > \delta_{yy} > \delta_{zz}$ in nearly empty silicalite to $\delta_{zz} > \delta_{xx} > \delta_{yy}$ when completely full, but the differences between the components are much larger at full occupancy than at nearly zero occupancy.

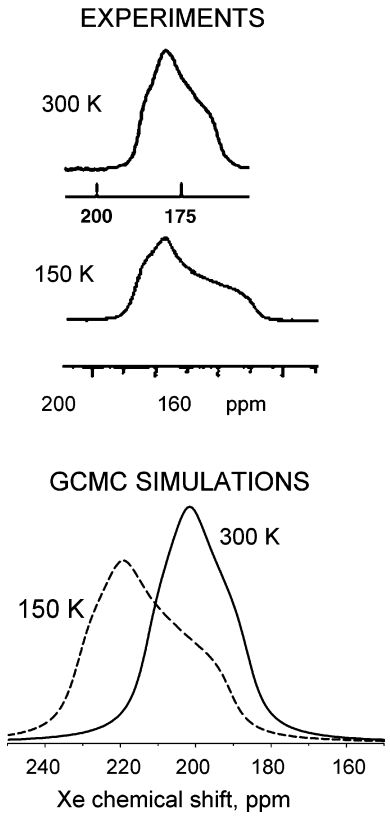

Figure 2. Line shapes of the ^{129}Xe NMR spectra at 300 and 150 K for polycrystalline silicalite at maximum occupancy (16 Xe atoms per unit cell) from GCMC simulations, compared with the line shapes at 300 K from ref 11 (reproduced with permission from the American Chemical Society) and at 150 K from ref 14 (reproduced with permission from the American Chemical Society).

Although experimental trends are well reproduced in Figure 2, at full occupancy the inadequacies of the pairwise potential and shielding functions used here (unchanged from our previous work) become more obvious. The three-body terms have not been included. It is known from our early work in Xe gas, at densities up to 250 times that of the number density at standard temperature and pressure, that the Xe chemical shift is not linear with density over the entire range.[26] When the Xe number density is in the range achieved in the channels and intersections of silicalite at full occupancy, the three-body terms and higher become significant. Since the density dependence of the many-body terms are opposite in sign to the two-body terms for Xe

(26) Jameson, A. K.; Jameson, C. J.; Gutowsky, H. S. *J. Chem. Phys.* **1970**, *53*, 2310−2321.

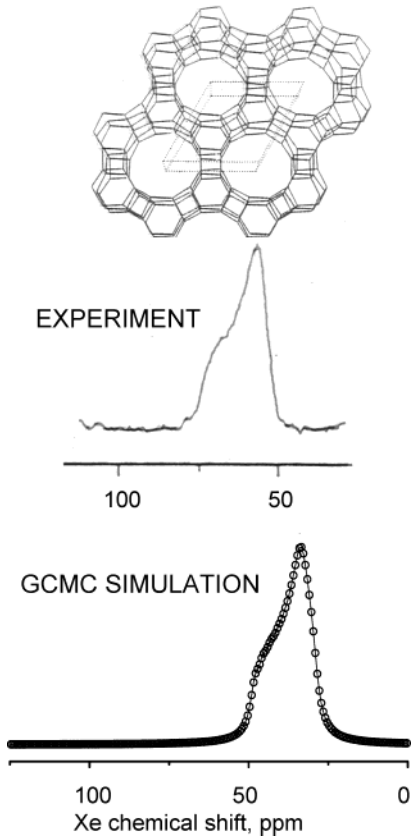

Figure 3. Theoretical ^{129}Xe NMR line shape in zeolite SSZ-24 at near-zero occupancy (0.04 Xe/UC at 300 K), compared with the experimental Xe NMR spectrum obtained in one scan using hyperpolarized Xe at 293 K from ref 28 (reproduced with permission from the American Chemical Society).

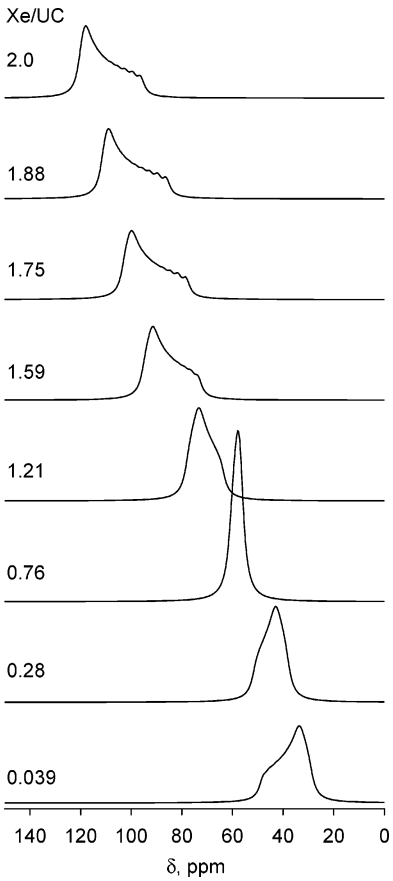

Figure 4. Theoretical ^{129}Xe NMR line shapes in zeolite SSZ-24 from GCMC simulations of Xe in a simulation box of 2 × 2 × 3 unit cells under periodic boundary conditions at 300 K.

gas (chemical shifts are not as large as linear extrapolation predicts), one should not expect quantitative agreement with the absolute magnitudes of the chemical shifts from experiment. This explanation does predict discrepancies in Figure 2 between the absolute shifts from experiment and from simulations in the correct direction (predicted shifts are larger than experimental). At low temperatures (150 K) the many-body terms become more significant than at room temperature.

b. SSZ-24. Finally, we apply the same Xe−O shielding functions and potential functions to another highly siliceous zeolite in which the channel walls consist of bridging oxygens with essentially the same electronic structure as in silicalite, (connected to two Si atoms) but is a zeolite with a simpler channel structure. The structure of SSZ-24, a hexagonal structure with straight channels along the short axis in the unit cell, a silica analogue of ALPO-5,[27] is shown in Figure 3. The channel opening is a T12 ring (i.e., made up of 12 Si atoms connected by bridging oxygen atoms), and the channel walls consist of fused T6 rings. The experimental Xe NMR spectrum of SSZ-24 at near-zero occupancy has been obtained in one scan by Moudrakovski et al. using hyperpolarized Xe.[28] This experimental spectrum is shown in Figure 3. The results of GCMC simulations using the same methods and parameters as for silicalite, using a simulation box of 2 × 2 × 3 unit cells under periodic boundary conditions, resulted in the spectra shown in Figures 3 and 4.

In Figure 3 we compare the results of a simulation with 0.04 Xe/unit cell at 300 K with the spectrum observed by Moudrakovski et al. at 293 K. We see that we reproduce the sign and the magnitude of the anisotropy of this axially symmetric average Xe shielding tensor. The nearly circular cross section of the channels in this zeolite makes it possible to predict the number of unique tensor components and the sign of the anisotropy, even without benefit of simulations.[29] The simulations provide $\delta_{zz} - \delta_{xx} = 20$ ppm, whereas the experimental anisotropy is about 25 ppm. The *zz* component is along the axis of the channel (*c* axis of the crystal). Our agreement with the absolute magnitudes of the shielding tensor components is only semiquantitative.

Grand canonical Monte Carlo simulations provide a prediction of the change of Xe line shape with increasing occupancy at constant temperature for a polycrystalline sample. This has not yet been observed experimentally in SSZ-24, but Xe line shapes in an organic channel of similar cross section have been investigated experimentally under variable Xe occupancy conditions by varying temperature and Xe mole fraction in the gas stream.[12,13] The theoretical spectra for Xe in SSZ-24 as a function of occupancy at 300 K are shown in Figure 4. Maximum occupancy found in the simulations is 2 Xe/unit cell. The systematic change in the anisotropy of the average Xe tensor from one sign to another with increasing occupancy, for

(27) Bialek, R.; Meier, W. M.; Davis, M.; Annen, M. J. *Zeolites* **1991**, *11*, 438−442.
(28) Moudrakovski, I. L.; Nossov, A.; Lang, S.; Breeze, S. R.; Ratcliffe, C. I.; Simard, B.; Santyr, G.; Ripmeester, J. A. *Chem. Mater.* **2000**, *12*, 1181−1183.
(29) Jameson, C. J.; de Dios, A. C. *J. Chem. Phys.* **2002**, *116*, 3805−3821.

example, $\delta_{||} > \delta_{\perp}$ at near-zero occupancy to $\delta_{\perp} > \delta_{||}$ at full occupancy, is a signature of a channel with a cross section having an aspect ratio very close to 1.

In addition, simulations at very low occupancy at 300, 250, 200, and 150 K permit the determination of the Xe−channel part of the tensor as a function of temperature. Each of the three components of the Xe−channel part of the chemical shift tensor decreases with decreasing temperature, by about 7 ppm in 150 deg.

4. Discussion

When two components are very similar for the nearly empty channel, as it was in the ALPO-11 case,[20] the Xe line shape observed in polycrystalline samples may seem to indicate an axially symmetric tensor, i.e., a channel cross section with aspect ratio very close to 1. At full Xe occupancy the tensor components have diverged and have become more clearly indicative of the cross-sectional symmetry of the channel. The Xe line shape at high occupancy is a more robust indicator of the aspect ratio of the cross section than is the line shape at nearly zero occupancy. This is due to the Xe−Xe dimer contributions to the observed tensor being typically larger than the Xe−O (or other Xe channel) contributions. In both the SSZ-24 and the silicalite example, the line shape at full occupancy using thermally polarized Xe can be just as good an indication of channel architecture as a near-zero-occupancy hyperpolarized Xe NMR spectrum. For example, in silicalite at full occupancy (Figure 2) there can be no doubt that this is not an axially symmetric tensor.

In a typical narrow-bore channel, with dimensions such that Xe atoms cannot pass each other in the channels, the tensor component whose average remains essentially constant from zero to full occupancy is the component which is along the axis of the channel. In the simulations in such systems, there are no contributions from Xe−Xe dimers whose centers lie in a plane perpendicular to the channel axis. Thus, the tensor component along the channel axis consists only of averages over Xe−O dimer contributions. Averaging in static channels (assumption of unchanged zeolite crystalline structure) results in only a slight increase in the Xe−O contributions to this tensor component with increasing Xe occupancy, and this component can be assigned to the channel axis direction with confidence. Such was the case with ALPO-11, where the Xe−Xe contributions to the tensor component along the direction of the channel remained small throughout the increasing occupancy of the channel.[15] The situation in SSZ-24 is somewhat different, although the component along the axis of the channel can still be assigned with confidence from the spectrum. The GCMC simulations show that the latter component does not remain constant with increasing Xe occupancy; it increases as the Xe−Xe contributions increase, although not as fast as the perpendicular component.

Due to the local nature of the chemical shift, only the nearest neighbors contribute significantly to the tensor components. Thus, a $XeXe_2$ model captures the essential behavior of Xe in highly occupied channels. The ab initio calculations in $XeXe_2$ at various geometries shed some light on the conditions under which the chemical shift tensor component along the direction of the channel can remain nearly constant as the occupancy approaches maximum.[29] For a given Xe−Xe distance, say 4.0 Å, for the middle Xe in $XeXe_2$, the chemical shift tensor component perpendicular to the bisector of the Xe−Xe−Xe angle (i.e., along the channel axis) increases very slowly (about 7 ppm) in going from 180° to 150°, and then increases much faster (about 40 ppm) in going from 150° to 120°.[29] This means that when the zigzag arrangement of Xe atoms in the highly occupied channel has an angle in the range 150°−180°; the chemical shift tensor component along the channel axis will change hardly at all with increasing Xe occupancy; at about 120° the same component can change significantly with increasing occupancy. We found the former case in ALPO-11 in previous work[15] and the latter case in SSZ-24 (a silica analogue of ALPO-5) in the present work. The cross-sectional area of the channel dictates whether the $XeXe_2$ groupings of atoms within the channel can achieve angles smaller than 150°−180°; groupings with smaller angles are less likely in smaller cross sections. With oxygen atoms assigned a nominal van der Waals radius of 1.35 Å, the ALPO-11 channel opening is an ellipse of 4.0 × 6.5 Å, the two types of silicalite channels have dimensions 5.5 × 5.1 Å and 5.3 × 5.6 Å, and the SSZ-24 opening has a diameter of 7.3 Å. Thus, it is easy to understand why the Xe chemical shift tensor component along the channel direction in ALPO-11 remains nearly unchanged with increasing Xe occupation, experimentally and theoretically. In SSZ-24 the simulations predict that the change in the tensor component along the channel direction is not as large as the perpendicular components, but is much larger than the approximately 5−8 ppm that was found in ALPO-11. Only in the larger diameter channels is it possible for the $XeXe_2$ groupings to achieve angles smaller than 150°−180°, permitting the component along the channel axis to change significantly in going from empty to full occupation. It is interesting to note that this is yet another signature of the channel architecture manifested in the Xe line shape.

The Xe one-body distributions at 300 K for Xe in SSZ-24 are shown in Figure 5. The one-body distribution functions reveal that, even at 300 K, the highest probability of finding the Xe is not right in the center (the axis) of the channel, but rather is in doughnut-shaped sweet spots along the channel, two per unit cell. The repeat distance for these sweet spots along the direction of the channel axis is 4.2 Å, whereas the r_{min} of the Xe−Xe potential function is 4.3627 Å and r_0 is 3.892 44 Å.[23] The high probability regions for the Xe atoms are in register with the network of fused T6 rings which make up the channel walls. Thus, there is a good fit and the maximum occupancy of 2 Xe atoms per unit cell is easily rationalized.

The chemical shift tensor at the zero-occupancy limit includes no Xe−Xe contributions; therefore, this serves as a good signature of the Xe−channel interactions. The predicted chemical shift behavior of a single Xe atom in a channel of SSZ-24 as a function of temperature is probably not very accurate for the quality of potential function that we have used. Nevertheless, the qualitative aspects of the predictions are expected to be reliable. The GCMC simulations find the following in the range 150−300 K: In a nearly empty channel all tensor components of the Xe chemical shift decrease with decreasing temperature. The one-body distribution function for one Xe in a channel at room temperature is similar to that shown in Figure 5. As the temperature goes down, the probability distribution function in

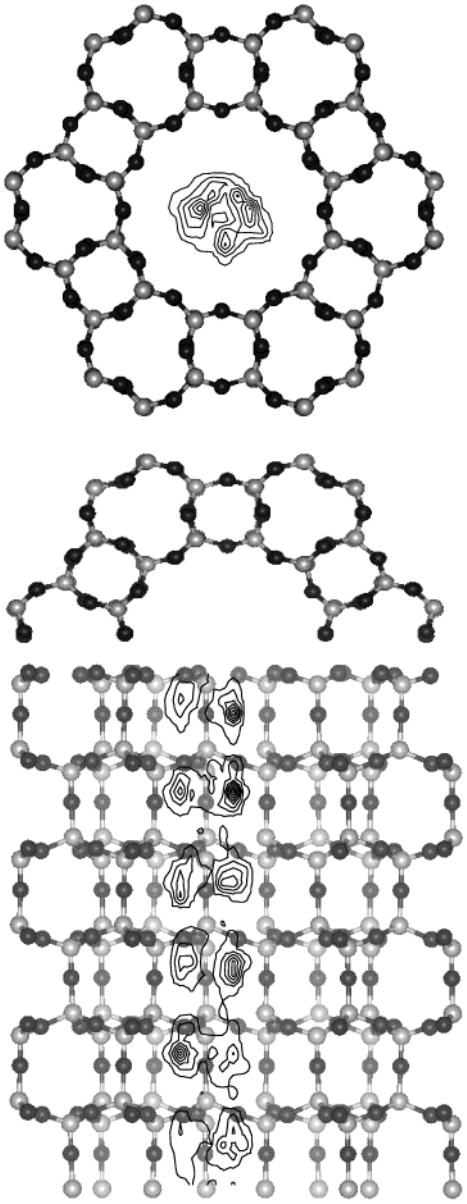

Figure 5. Probability distribution of the Xe within the channel of SSZ-24 at 300 K at 94% of maximum Xe occupancy. The two views are (top) on a plane perpendicular to the *c* axis of the crystal, showing a cross section of a channel, and (bottom) on a plane parallel to the axis of a channel.

the channel cross section becomes more localized. With increasing temperatures, the probability distribution function in the channel cross section spreads out, so that the probability of finding Xe closer to the center of the channel (farther away from the wall atoms) increases; the latter correspond to smaller chemical shift values. The probability of finding Xe closer to the wall atoms also increases; these correspond to larger chemical shift values. The interplay between these two trends leads to the temperature dependence being sensitive to the size of the channel. With a small-diameter channel, spending more time closer to the center does not permit the Xe to be much farther away from the channel walls. The distance dependence of the Xe shielding is not linear: Xe chemical shifts increase rapidly at shorter distances between Xe and neighbor atoms. Thus, the average Xe chemical shift increases with increasing temperature at the zero-occupancy limit when the channels have small cross sections. The opposite behavior can occur when the channel cross section is large enough. Somewhere between the two extremes the Xe−channel contributions to the chemical shift can be essentially temperature independent. The predicted behavior from the GCMC simulations in SSZ-24 is as follows: All tensor components increase somewhat with increasing temperature from 150 to 300 K at the zero-occupancy limit. This is opposite the observed trend for a Xe atom in zeolite NaY with its supercages, for example.[30]

Now let us consider the temperature dependence in the fully occupied channels. This would be dominated by the Xe−Xe contributions. This, too, is a signature of the size of the channel. If the channel is large enough, the Xe−Xe average distances can decrease with increasing temperature as the Xe probability distribution spreads out. On the other hand, if the channel has a small cross section, there is no space for the Xe atoms to move away from each other, and increasing temperature only permits sampling of the repulsive regions of the Xe−Xe intermolecular potential, which regions correspond to higher chemical shifts. For example, the Xe_8 peak which corresponds to the full cages of zeolite NaA exhibited chemical shifts sharply increasing with increasing temperature in the range 175−360 K.[31] In SSZ-24, our GCMC simulations find all the average tensor components are smaller at 150 K than at 300 K at nearly identical occupancies (1.89 and 1.88 Xe/unit cell, respectively). The one-body distribution at 150 K (not shown here) is sharper, less spread out than the one shown in Figure 5 at 300 K, with the Xe atoms having the highest probability of being found close to the minimum energy positions. The Xe atom's incursions into the walls of the channel at 150 K are not as severe as at 300 K; thus the Xe−O contributions are not as large as at 300 K. Likewise, the Xe atom's incursions into the Xe−Xe repulsive regions are not as severe at 150 K as at 300 K; thus the Xe−Xe contributions are not as large as at 300 K. Taken together, these effects lead to each chemical shift tensor component being smaller at 150 K than at 300 K, with the total isotropic chemical shift at 94% occupancy decreasing by about 13 ppm in the 150 deg decrease in temperature. The experiments to verify these predictions are not yet available. This predicted temperature dependence for Xe in SSZ-24 channels at near-maximum occupancy is opposite that predicted (and observed) in silicalite.

5. Conclusions

We have successfully reproduced the essential features of the experimental results on Xe in single-crystal and polycrystalline silicalite at various occupancies and temperatures from experiments conducted in two independent laboratories, using the same set of Xe−O shielding functions and Xe−O potential functions throughout. The GCMC simulations permit the assignment of the smallest tensor component to the direction along the axis of the straight channels.

We also use the same set of shielding and potential parameters to predict the Xe NMR line shapes in SSZ-24 as a function of occupancy at constant temperature. The theoretical line shape at nearly zero Xe occupancy in SSZ-24 compares very favorably with the experimental line shape observed in one scan using hyperpolarized Xe. The predicted line shape changes for Xe in SSZ-24 upon increasing occupancy and with changing temper-

(30) Labouriau, A.; Pietrass, T.; Weber, W. A.; Gates, B. C.; Earl, W. L. *J. Phys. Chem. B* **1999**, *103*, 4323−4329.
(31) Jameson, C. J.; Jameson, A. K.; Baello, B. I.; Lim, H. M. *J. Chem. Phys.* **1994**, *100*, 5965−5976.

ature can be understood with the help of the one-body distribution functions. The Xe−Xe contributions account for most of the changes with increasing Xe occupancy predicted for the average Xe tensor components in both silicalite and SSZ-24. The significant change of the tensor component along the channel axis is a signature of a channel cross section large enough to permit the $XeXe_2$ groupings in the channels at high occupancy to achieve angles smaller than 150°−180°. The temperature dependence at the zero-occupancy limit and also at the full-occupancy limit are shown to be signatures of the size of the channel, in the case of one type of channel running along only one dimension of the crystal, as in SSZ-24. The situation in systems with two types of channels and intersections, such as silicalite, is more complex and less amenable to qualitative predictions. Nevertheless, in the latter case, the GCMC simulations do provide the correct temperature dependence of each tensor component.

The Xe line shape at high occupancy is a more robust indicator of the aspect ratio of the cross section of the channel than is the line shape at nearly zero occupancy. This is due to the Xe−Xe dimer contributions to the observed tensor being usually larger than the Xe−O (or other Xe−channel) contributions. Thus, the line shape at full occupancy using thermally polarized Xe can be just as good an indication of channel architecture as a near-zero occupancy hyperpolarized Xe NMR spectrum. The electronic structure of the channel atoms is, however, most clearly indicated by the Xe spectrum in the nearly empty channel. The latter experiment is the ultimate test of Xe−channel intermolecular interactions, incorporating both the shielding and the potential functions.

Acknowledgment. This research has been supported by the National Science Foundation (Grant CHE-9979259).

JA040012A